Reaction of Negatively-Charged Clusters of Carbon Dioxide with CH_3I: Formation of Novel Molecular Anion $CH_3CO_2I^-$

Tatsuya Tsukuda,[†] Morihisa Saeki,[†] Suehiro Iwata,[‡] and Takashi Nagata*[,†,‡]

Department of Basic Science, Graduate School of Arts and Sciences, The University of Tokyo, Komaba, Meguro-ku, Tokyo 153, Japan, and Institute for Molecular Science, Myodaiji, Okazaki 444, Japan

Received: March 10, 1997; In Final Form: May 9, 1997[⊗]

Reaction of negatively-charged clusters of carbon dioxide $(CO_2)_N^-$ with CH_3I results in the formation of anions with the formulae $[(CO_2)_nCH_3I]^-$, $[(CO_2)_nCH_3]^-$, and $[(CO_2)_nI]^-$. The product mass spectrum of $[(CO_2)_nCH_3I]^-$ displays a distinct bimodal distribution; $[(CO_2)_nCH_3I]^-$ with $n = 1-3$ and $n \geq 7$ are observed, while those with $n = 4-6$ are not detected. Photoelectron spectroscopy of $[(CO_2)_nCH_3I]^-$ reveals that $[(CO_2)CH_3I]^-$ is formed as the core of $[(CO_2)_nCH_3I]^-$ with $1 \leq n \leq 3$ while CO_2^- is the core for $n \geq 7$. The $[(CO_2)CH_3I]^-$ core also behaves as chromophore, which absorbs a 532 nm photon to dissociate into $CH_3CO_2^- + I$ or $CH_3CO_2 + I^-$ channels. The chemical identity of $[(CO_2)CH_3I]^-$ is probed by the combination of photodissociation and photoelectron spectroscopic techniques. *Ab initio* calculations have also been performed to examine the geometrical and electronic structures of $[(CO_2)CH_3I]^-$. We conclude from these results that $[(CO_2)CH_3I]^-$ is composed as a molecular anion of acetyloxy iodide, $CH_3CO_2I^-$, where the acetyloxyl framework binds the I atom through an O−I bond to share the excess electron. The formation mechanism of $CH_3CO_2I^-$ is discussed on the basis of the observed steric effects on the reaction.

Introduction

Since the pioneer work of Klots and Compton,[1] negatively-charged clusters of carbon dioxide, $(CO_2)_n^-$, have been drawing much attention as a benchmark system for the study of formations, stabilities, and structures of molecular cluster anions.[2−15] The attention derives mostly from the fundamental question regarding the electronic properties of $(CO_2)_n^-$: i.e., how the aggregates of CO_2 can bind excess electrons, in contrast to the fact that CO_2^- is an unstable species with the lifetime against autodetachment of less than 100 μs.[16] As for $(CO_2)_2^-$, Fleischman and Jordan have theoretically proposed two possible forms of stable structure: $C_2O_4^-$ molecular anion with D_{2d} symmetry and $[CO_2^-\cdots CO_2]$ ion−solvent complex having C_s symmetry.[12] They also predicted that these two forms of $(CO_2)_2^-$ are quite close in energy but have different vertical detachment energies, with which they are distinguishable by photoelectron spectroscopy.[13] DeLuca et al. have shown in their photoelectron spectroscopic study that $C_2O_4^-$ is formed as the anionic core in $(CO_2)_n^-$ with the size of $2 \leq n \leq 5$, while the excess electron is localized on a CO_2^- constituent for $n \geq 7$.[14] More recently, Tsukuda et al. have extended the measurements of the photoelectron spectra of $(CO_2)_n^-$ up to $n = 16$ and revealed the correlation between the core formation and the relative stabilities of $(CO_2)_n^-$ clusters.[15] Although these studies have shed light on the fundamental properties of $(CO_2)_n^-$, such as geometrical and electronic structures, little is known about chemical properties of $(CO_2)_n^-$. To our knowledge, there have been reports on photoexcitation[17] and collisional excitation[18] of $(CO_2)_n^-$. In both cases, the only process observed is evaporative loss of the CO_2 solvents. From a point of view that $(CO_2)_n^-$ can be regarded as gas-phase analogue to $^\bullet CO_2^-$ radical anion in the condensed phase, one might refer to reactions of $^\bullet CO_2^-$ in solutions or in crystalline matrices. The reactions of $^\bullet CO_2^-$ with various organic and inorganic compounds have been investigated in the condensed phase by pulse radiolysis and flash photolysis.[19] In these reactions, $^\bullet CO_2^-$ acts as a strongly reducing species; reaction proceeds as $^\bullet CO_2^- + M \rightarrow CO_2 + {}^\bullet M^-$. In the electrochemical processes, reductive activation of CO_2 in the presence of alkyl halides (RX) yields fixation products, such as RCO_2R, R_2CO_3.[20]

In our previous study, we have reported the formation of anions with the formula $[(CO_2)_nCH_3I]^-$ in the gas-phase reactions of $(CO_2)_n^-$ with methyl iodide.[21] In that study, an attempt was made to measure the photoelectron spectra of the product $[(CO_2)_nCH_3I]^-$ at 355 nm (3.49 eV). The measurement revealed that the photoelectron band of $[(CO_2)_nCH_3I]^-$ is located above the cutoff energy of our photoelectron spectrometer ($\approx$3.25 eV) and that $[(CO_2)_nCH_3I]^-$ with $n = 1-3$ contain a chromophore that photodissociates at 355 nm. From these observations it was concluded that $[(CO_2)CH_3I]^-$ forms the anionic core of $[(CO_2)_nCH_3I]^-$ with $n = 1-3$ and that $[(CO_2)CH_3I]^-$ possesses a vertical detachment energy (VDE) greater than 3.25 eV. The large VDE value implies that the excess electron is delocalized to a considerable extent in $[(CO_2)CH_3I]^-$. Considering the fact that both acetyloxyl radical, CH_3CO_2, and I atom have electron affinities of $\approx$3 eV (EA(CH_3CO_2) = 3.07 eV,[22] EA(I) = 3.06 eV[23]), we have proposed an acetate−iodine complex $[CH_3CO_2\cdots I]^-$ as the possible structure of $[(CO_2)CH_3I]^-$. However, the chemical identity, geometrical structures, and electronic properties of $[(CO_2)CH_3I]^-$ still remain unsettled. In the present study, we have reexamined photoelectron spectra of the product anions in the reaction of $(CO_2)_n^-$ with CH_3I by employing a higher photon energy (4.66 eV). The measurement yields photoelectron spectra for $[(CO_2)_nCH_3I]^-$ with $n = 1-3$ and $7-9$, with which we have determined the VDE values of $[(CO_2)_nCH_3I]^-$. Since our previous study showed the existence of a photoabsorption band in $[(CO_2)_nCH_3I]^-$ below the photodetachment threshold, photofragmentation of $[(CO_2)_nCH_3I]^-$ has also been investigated in the present study to obtain information on the chromophoric core of $[(CO_2)_nCH_3I]^-$. In the photodissociation experiment, photofragments from

* Corresponding author. E-mail, nagata@laserchem.c.u-tokyo.ac.jp; fax, +81-3-5454-4353.
† The University of Tokyo.
‡ Institute for Molecular Science.
⊗ Abstract published in *Advance ACS Abstracts,* June 15, 1997.

S1089-5639(97)00871-2 CCC: $14.00

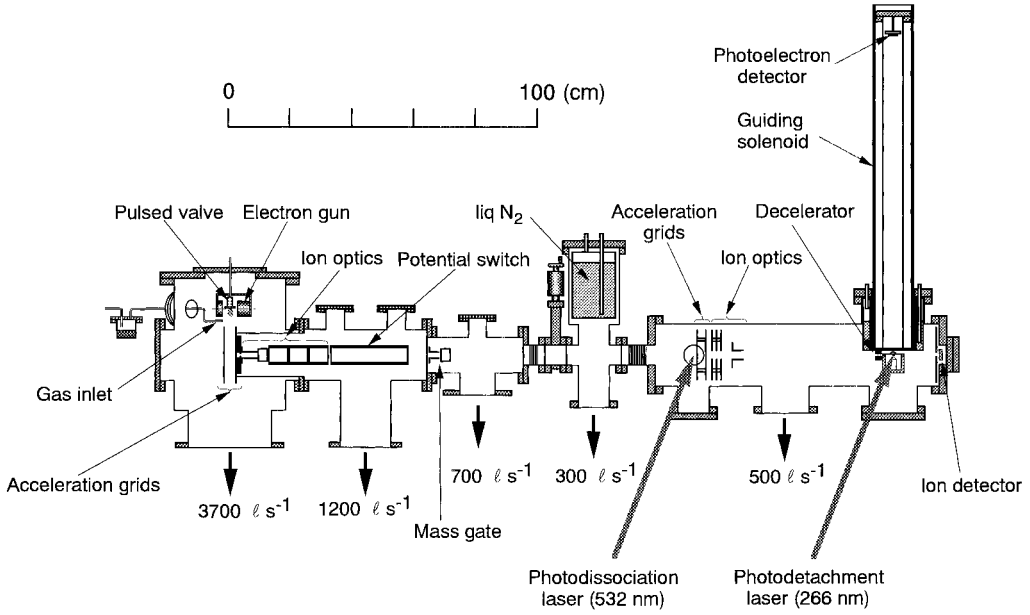

Figure 1. Schematic of the experimental apparatus.

$[(CO_2)_nCH_3I]^-$ were mass analyzed; the fragmentation pattern not only serves as a "fingerprint" to identify the chromophore in the larger homologues but also reflects the chemical bondings in the chromophoric core. While photoelectron spectroscopy and photodissociation techniques are useful to probe the electronic structures of the product anions and to identify their chromophoric cores, they become even more powerful when combined; measurement of photoelectron spectra of the photofragments from $[(CO_2)_nCH_3I]^-$ is used here to examine the chemical identity of $[(CO_2)CH_3I]^-$. To aid in understanding these experimental findings, *ab initio* calculations have been performed on the geometrical structures and electronic properties of $[CH_3CO_2\cdots I]^-$. We also report on the reactions of $(CO_2)_n^-$ with other alkyl iodides, such as C_2H_5I and 2-C_3H_7I. The reaction mechanism operative in the $(CO_2)_n^- + CH_3I$ system is discussed on the basis of these experimental and theoretical findings.

Experimental Section

The schematic of the experimental apparatus is shown in Figure 1. The apparatus consists of a cluster ion source, a tandem time-of-flight (TOF) mass spectrometer, and a photoelectron spectrometer. The $(CO_2)_N^-$ reactants are prepared by electron attachment to neutral CO_2 clusters in an electron-impact ionized free jet;[24] the CO_2 clusters are formed by pulsed expansion of pure CO_2 gas at the stagnation pressure of 1−2 atm. An injection of an electron beam of 250 eV into the supersonic expansion produces secondary slow electrons, which are attached to the preformed CO_2 clusters. The CH_3I sample (Kanto Chemicals, >98% purity) is introduced into the source chamber through an effusive nozzle. The pressure of the chamber increases from $\approx 1 \times 10^{-7}$ to $\approx 2 \times 10^{-5}$ Torr when the CO_2 jet is on and up to $\approx 1 \times 10^{-4}$ Torr with the introduction of CH_3I gas. The $(CO_2)_N^-$ clusters react with CH_3I while drifting in the source chamber. The product anions are then extracted at ≈15 cm downstream the nozzle, perpendicularly to the initial beam direction, by applying a pulsed electric field of 20 V cm^{-1}. The anions are further accelerated to ≈500 eV, mass analyzed by a 2.3-m long TOF mass spectrometer, and detected by a dual microchannel plate (Hamamatsu MCP F4655-10). The resolution of the TOF mass spectrometer is $m/\Delta m \approx 500$. The signals from the MCP are amplified and accumulated by a 500-MHz digitizing oscilloscope (Tektronix TDS520A).

Three types of measurements were performed in the present study: measurement of photofragment spectra and photoelectron spectra of the product anions and measurement of photoelectron spectra of the photofragment anions. In the photodissociation measurement, the apparatus is used as a collinear tandem TOF spectrometer. The cluster anions of interest are spatially and temporally focused at the point 1.54 m downstream the first acceleration grids. At the focus the anions are crossed with the second harmonic (532 nm) of a pulsed Nd:YAG laser (Quanta-Ray GCR-12S). The laser fluence used is in the range 60−70 mJ $pulse^{-1}$ cm^{-2}. The photofragments are then reaccelerated by a pulsed electric field (1 kV, 700 ns duration) at the second acceleration assembly. The 0.8-m flight path to the MCP detector serves as the second mass analyzer. The photofragment signals are accumulated by the digitizing oscilloscope typically for 100−1000 laser shots.

In photoelectron measurement, mass selection is achieved by a pulsed beam deflector (mass gate) prior to photodetachment. The mass-selected cluster anions are then admitted into the photoelectron chamber. The chamber is evacuated with a series of turbo molecular pumps (500 *l*/s + 50 *l*/s), and the ambient pressure is kept at $\approx 3 \times 10^{-10}$ Torr under typical operation conditions. At the photodetachment region, the fourth harmonic (266 nm) of the Nd:YAG laser is timed to intersect the mass-selected ion bunch. The laser fluence is kept within 5 mJ $pulse^{-1}$ cm^{-2}. The kinetic energies of the photoelectrons are measured by a magnetic-bottle type electron spectrometer;[25] the electrons are detached in a strong inhomogeneous magnetic field (≈1000 G) and further guided by a weak field (≈10 G) down to a detector installed at the end of a 1-m flight tube. The 1000 G magnetic field is generated by a cylindrical permanent magnet with a soft iron tip to enhance the field.[26,27] The photoelectrons are detected by a double thickness microsphere plate with a 27-mm diameter (El-Mul Z033DA) and counted by a multichannel scaler/averager (Stanford Research SR430). The photoelectron spectra in this study were obtained without decelerating the cluster anions, because the deceleration weakens the signal intensities and because no significant change is observed in the spectral profile with the deceleration down to 50 eV. Each spectrum presented in this paper represents an accumulation of 25000−50000 laser shots with background subtraction. The measured electron kinetic energy is calibrated against the known photoelectron band of I^- and $I^-(CO_2)$ anions.[28] The energy

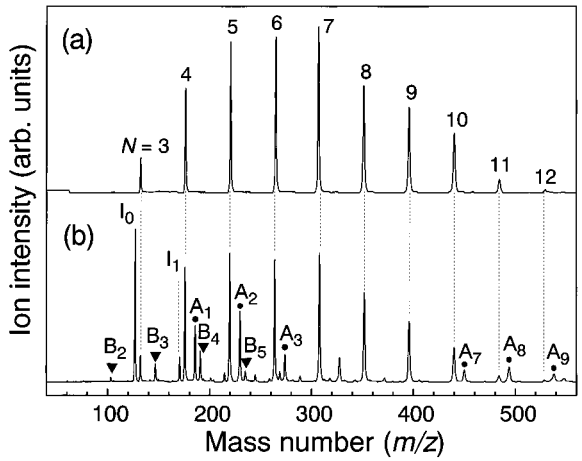

Figure 2. Mass spectra of (a) the $(CO_2)_N^-$ reactants and (b) product anions in the reaction of $(CO_2)_N^-$ with CH_3I. The mass peaks for the product anions are interspersed between the unreacted $(CO_2)_N^-$ peaks. The labels A_n, B_n, and I_n represent the species with the formulae $[(CO_2)_nCH_3I]^-$, $[(CO_2)_nCH_3]^-$, and $[(CO_2)_nI]^-$, respectively.

resolution of the spectrometer is ≈100 meV at the electron kinetic energy of 1 eV.

The present experimental setup allows us to measure the photoelectron spectra of the photofragments. In the photodissociation−photoelectron measurement, two sets of Q-switched Nd:YAG lasers are used. Mass-selected anions are photodissociated at the focus of the first TOF spectrometer by applying the second harmonic of a Nd:YAG laser (Quanta-Ray GCR-130). The photofragment anions are mass analyzed by the second TOF spectrometer, and the anions of interest are chosen by the time delay between the second pulse acceleration and the irradiation of the 266-nm photodetachment laser. The procedure of data acquisition is identical with that in the photoelectron measurement.

Results

A. Product Anions of $(CO_2)_N^-$ + CH_3I Reaction. The upper trace of Figure 2 shows a typical mass spectrum of the $(CO_2)_N^-$ reactants. When the CH_3I reagent is introduced into the source chamber, mass peaks of the product anions emerge in the spectrum, as shown in the lower trace of Figure 2. In addition to the unreacted $(CO_2)_N^-$, anions with the formulae $[(CO_2)_nCH_3I]^-$, $[(CO_2)_nI]^-$, and $[(CO_2)_nCH_3]^-$ (A_n, I_n, and B_n in the panel, respectively) are observed in the spectrum. The mass assignments were confirmed by using CD_3I, instead of CH_3I, as a reagent. It is apparent from the observed mass spectrum that the distribution of $[(CO_2)_nCH_3I]^-$ exhibits a bimodal behavior; the cluster anions with $n = 1-3$ and $n \geq 7$ are observed while those with $n = 4-6$ are missing. The population of $[(CO_2)_nI]^-$ decreases rapidly with the increase in the cluster size, while $[(CO_2)_nCH_3]^-$ anions are populated in the range $2 \leq n \leq 7$ with the maximum at $n = 4$. As discussed in our previous work,[21] these product anions arise from the collisional reactions of existing $(CO_2)_N^-$ clusters in the ionized jet with ambient CH_3I gas:

$$(CO_2)_N^- + CH_3I \rightarrow [(CO_2)_nCH_3I]^- + (N-n)CO_2 \quad (1a)$$

$$\rightarrow [(CO_2)_nI]^- + CH_3 + (N-n)CO_2 \quad (1b)$$

$$\rightarrow [(CO_2)_nCH_3]^- + I + (N-n)CO_2 \quad (1c)$$

In order to check on the possibility that the product anions are formed via the electron capture by neutral clusters, such as

$$(CO_2)_M \xrightarrow{CH_3I} (CO_2)_NCH_3I \xrightarrow{e^-} \text{product anions} \quad (2)$$

we have examined the anionic species formed in the electron attachment to neutral $(CO_2)_m(CH_3I)_n$ clusters. The $(CO_2)_m(CH_3I)_n$ clusters were produced by a supersonic expansion of CO_2 gas containing a small amount of CH_3I. No anions with formulae $[(CO_2)_nCH_3I]^-$ or $[(CO_2)_nCH_3]^-$ were detected, while a series of $[(CO_2)_nI]^-$ was observed as a dominant product. The product distributions of $[(CO_2)_nI]^-$, however, differ significantly from those in the $(CO_2)_N^- + CH_3I$ reactions; the distribution extends up to $n = 10$ with a maximum at $n = 3$ in the dissociative electron attachment to $(CO_2)_m(CH_3I)_n$. From these observations, it can be inferred that the product anions, $[(CO_2)_nCH_3I]^-$, $[(CO_2)_nI]^-$, and $[(CO_2)_nCH_3]^-$, arise primarily from the collisional reactions (processes 1a−1c), although we cannot completely neglect the contribution from process 2 as to the formation of $[(CO_2)_nI]^-$.

As the reactions of $(CO_2)_N^-$ with CH_3I occur downstream of the supersonic expansion, one might expect that the nascent product distributions are somewhat smeared by subsequent nucleation via ion−molecule collisions. To evaluate qualitatively the effect of the ion−molecule collisions, we have examined the product mass distributions by changing the stagnation pressure of CO_2 gas and electron-beam nozzle distance. Although the relative intensities of the product mass peaks were observed to depend slightly on the source conditions, the $[(CO_2)_nCH_3I]^-$ peaks with $n = 4-6$ never appeared in the mass spectra. The implication is that subsequent ion−molecule collisions are largely unimportant to the product mass distributions. Thus we infer that the product distributions observed are determined mostly by the reaction scheme.

B. Photodissociation of $[(CO_2)_nCH_3I]^-$. In our previous study we found that an intense narrow peak at $E_b = 3.06$ eV dominates the photoelectron spectra of $[(CO_2)_nCH_3I]^-$ ($1 \leq n \leq 3$) measured at 355 nm.[21] The peak is ascribed to $I(^2P_{3/2})$, which arises from the two-photon process:

$$[(CO_2)_nCH_3I]^- + h\nu\ (355\ \text{nm}) \rightarrow I^- + \text{neutral fragments} \quad (3)$$

$$I^- + h\nu\ (355\ \text{nm}) \rightarrow I(^2P_{3/2}) + e^- \quad (4)$$

This finding indicates that a photoabsorption band in $[(CO_2)_nCH_3I]^-$ ($1 \leq n \leq 3$) is located well below the vertical photodetachment energy and that the relevant upper state is dissociative. In the present study we have mass analyzed the photofragments from $[(CO_2)_nCH_3I]^-$ by using the tandem TOF arrangement. Preliminary measurements of the photofragment intensities in the 345−520 nm range showed that the photodissociation cross section reaches a maximum around 410 nm and decreases rapidly in the shorter wavelengths due probably to the onset of photodetachment channel. Figure 3 displays photofragment mass spectra of $[(CO_2)_nCH_3I]^-$ ($1 \leq n \leq 3$) measured at 532 nm. The $[(CO_2)CH_3I]^-$ spectrum displays two peaks at $m/e = 59$ and 127, which are assigned to $CH_3CO_2^-$ and I^-, respectively. It appears that the following channels compete with each other in the photodissociation of $[(CO_2)CH_3I]^-$ at 532 nm:

$$[(CO_2)CH_3I]^- + h\nu\ (532\ \text{nm}) \rightarrow CH_3CO_2^- + I \quad (5a)$$

$$\rightarrow CH_3CO_2 + I^- \quad (5b)$$

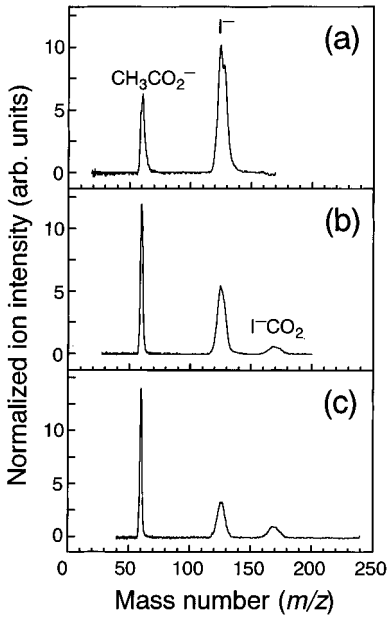

Figure 3. Photofragment mass spectra resulting from the 532 nm photodissociation of (a) $[(CO_2)CH_3I]^-$, (b) $[(CO_2)_2CH_3I]^-$, and (c) $[(CO_2)_3CH_3I]^-$. The ordinate scale is given such as to assign 10 units to the I^- fragment peak from $[(CO_2)CH_3I]^-$.

The spectra of $[(CO_2)_nCH_3I]^-$ with $n = 2$ and 3 demonstrate that the branching fraction for process 5a increases with the number of the CO_2 solvents. For $[(CO_2)_nCH_3I]^-$ with $n = 2$ and 3, $[(CO_2)I]^-$ is also observed as a photoproduct, which is formed as

$$[(CO_2)_nCH_3I]^- + h\nu\ (532\ \text{nm}) \rightarrow [(CO_2)I]^- + CH_3CO_2 + (n-2)\ CO_2 \quad (6)$$

No fragment was detected when the larger $[(CO_2)_nCH_3I]^-$ with $7 \leq n \leq 9$ are irradiated by 355 or 532 nm photons.

C. Photoelectron Spectra of Product Anions. Figure 4 shows photoelectron spectra of $[(CO_2)_nCH_3I]^-$ with $n = 1-3$ (left panel) and those with $n = 7-9$ (right panel) measured at 266 nm (4.66 eV). In these spectra, the photoelectron counts are plotted as a function of the electron binding energy defined as $E_b = h\nu - E_k$, where $h\nu$ and E_k represent the photon energy and the kinetic energy of the photoelectrons, respectively. An overview of these photoelectron spectra shows qualitatively that (1) the band profiles for $[(CO_2)_nCH_3I]^-$ with $1 \leq n \leq 3$ quite differ from those for $7 \leq n \leq 9$: there seems to be at least two peaks in the spectra for $1 \leq n \leq 3$, while the spectra for $7 \leq n \leq 9$ consist of a structureless single broad peak, and that (2) the electron binding energy does not increase monotonically with the cluster size: the $[(CO_2)CH_3I]^-$ band peaks around 3.6 eV, and the maximum shifts toward higher binding energies with increase in the cluster size up to $n = 3$, while the band maximum for $n = 7$ is located at $\approx$3 eV. The maxima of the photoelectron bands are interpreted as vertical detachment energies (VDEs) of the cluster anions. To determine the VDE and fwhm values quantitatively, the spectral profiles are fitted to a Gaussian function by a nonlinear least-squares method, where the band contour is expressed as

$$I(E_b) = C \exp[-(E_b - E_0)^2/\delta^2] \quad (7)$$

where E_0 corresponds to VDE and δ is related to the spectral width by fwhm $= 2(\ln 2)^{1/2}\delta$. Although the photoelectron band for $1 \leq n \leq 3$ has a second peak in the higher electron binding energies, the first band located in the lower energies is well

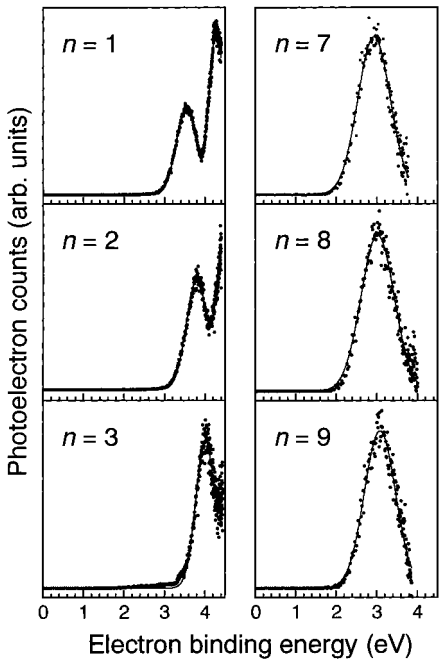

Figure 4. Photoelectron spectra of $[(CO_2)_nCH_3I]^-$ measured at the photon energy of 4.66 eV. Dots represent the experimental data. Best-fit profiles by assuming a Gaussian function are shown by solid lines (see eq 7). Note that the spectral features for $n = 1-3$ (left panel) differ from those for $n = 7-9$ (right panel) significantly.

TABLE 1: Vertical Detachment Energies and fwhm Values Determined from the $[(CO_2)_nCH_3I]^-$ Photoelectron Bands

n	VDE (eV)	fwhm (eV)
1	3.53 (0.02)[a]	0.57 (0.03)
2	3.79 (0.02)	0.60 (0.03)
3	4.01 (0.02)	0.54 (0.02)
7	2.94 (0.02)	0.94 (0.04)
8	3.02 (0.02)	0.95 (0.06)
9	3.09 (0.02)	0.92 (0.04)

[a] Numbers in parentheses indicate errors in derived quantities.

represented by a Gaussian function given by eq 7. The VDE and fwhm values thus determined for $[(CO_2)_nCH_3I]^-$ are listed in Table 1. The VDE value for $n = 1$ is determined to be 3.53 $\pm$ 0.02 eV. From $n = 1-3$, the value increases by 0.25−0.3 eV with the addition of another CO_2 molecule. At $n = 7$, the VDE value decreases down to 2.94 $\pm$ 0.02 eV. For $n \geq 7$, the increment in VDE with each additional CO_2 molecule is less than 0.1 eV. The width of the photoelectron bands for $1 \leq n \leq 3$ is in the range 0.5−0.6 eV, narrower than that for $7 \leq n \leq 9$.

Figure 5 displays photoelectron spectra of the product anions having stoichiometries $[(CO_2)_nCH_3]^-$ ($n = 2$, 3) and $[(CO_2)_nI]^-$ ($n = 0$, 1). The $[(CO_2)_2CH_3]^-$ spectrum consists of a broad peak with a shoulder in the high-energy side. The photoelectron spectrum of $[(CO_2)I]^-$ agrees well with that of $I^-(CO_2)$ reported by Arnold et al.[28] This allows us to identify the $[(CO_2)_nI]^-$ product anions with $I^-(CO_2)_n$.

Discussion

A. Electronic Structures of $[(CO_2)_nCH_3I]^-$. The experimental findings in the photodissociation and photoelectron measurements are summarized here: (1) $[(CO_2)_nCH_3I]^-$ with $n = 1-3$ possess a photoabsorption band well below the detachment threshold and photoexcitation leads to the production of either $CH_3CO_2^-$ or I^-, while photodetachment is the only photodestruction process for the larger members of $[(CO_2)_nCH_3I]^-$

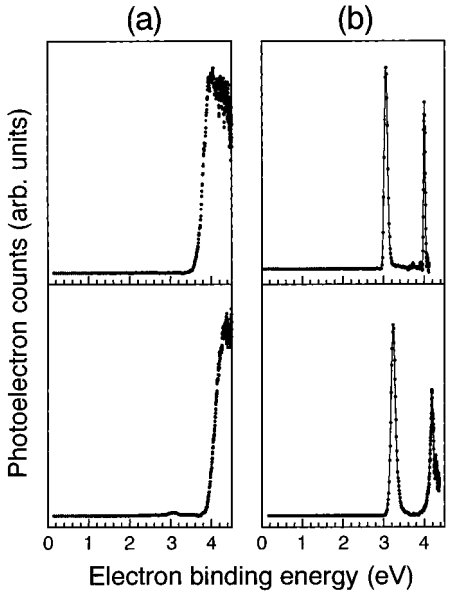

Figure 5. Photoelectron spectra of $[(CO_2)_nCH_3]^-$ and $[(CO_2)_nI]^-$ measured at the photon energy of 4.66 eV. (a) $[(CO_2)_nCH_3]^-$; the top panel is for $n = 2$ and the bottom for $n = 3$. (b) $[(CO_2)_nI]^-$; the top panel is for $n = 0$ and the bottom for $n = 1$.

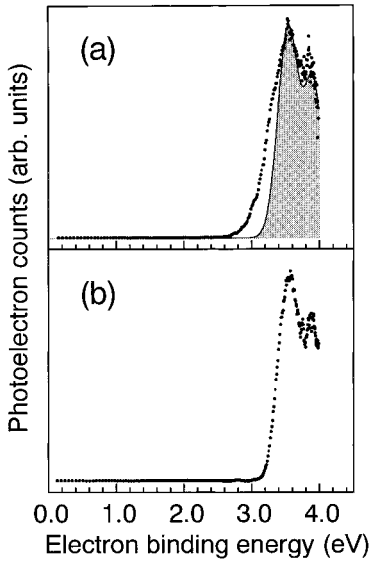

Figure 6. Photoelectron spectra of (a) the $CH_3CO_2^-$ species produced in the 532 nm photodissociation of $[(CO_2)_2CH_3I]^-$ and (b) an internally cold acetate anion formed via the dissociative electron attachment on acetic anhydride in the supersonic beam. The shaded area in panel a represents the copy of the acetate band profile. The low-energy tail of the $CH_3CO_2^-$ band is ascribable to vibrational hot bands.

with $n \geq 7$; (2) the vertical detachment energy of $[(CO_2)_nCH_3I]^-$ does not increase monotonically with the cluster size. The VDE values of $[(CO_2)_nCH_3I]^-$ with $n = 1-3$ are in the range of 3.53−4.01 eV, while those of the larger members with $n = 7-9$ are in the range of 2.94−3.09 eV.

The results obtained in the photodissociation experiments suggest that $[(CO_2)CH_3I]^-$ contains an acetyloxyl framework, CH_3CO_2. Within this context, $[(CO_2)CH_3I]^-$ can be rewritten as $[CH_3CO_2\cdots I]^-$. As the adiabatic electron affinity of acetyloxyl radical (3.07 eV[22]) is almost equal to that of iodine atom (3.06 eV[23]), two dissociation channels, $[CH_3CO_2\cdots I]^- \rightarrow CH_3CO_2^- + I$ and $[CH_3CO_2\cdots I]^- \rightarrow CH_3CO_2 + I^-$, are almost isoenergetic. The appearance of both $CH_3CO_2^-$ and I^- fragments in the photodissociation spectrum of $[(CO_2)CH_3I]^-$ (Figure 3a) is consistent with the energetics. In order to prove the chemical identity of the $CH_3CO_2^-$ ($m/e = 59$) photofragment, an effort was made to measure the photoelectron spectrum of $CH_3CO_2^-$ produced in the photodissociation of $[(CO_2)CH_3I]^-$ and to compare the spectrum with that of acetate. The fragment intensity, however, turned out to be insufficient to obtain a photoelectron spectrum with substantial intensities. Instead, we have measured the photoelectron spectrum of $CH_3CO_2^-$ from $[(CO_2)_2CH_3I]^-$, which provides more intense fragment signals in the 532-nm photodissociation. While the parent species are different, it does not prevent us from furthering the discussion because the photofragment originates from the $[CH_3CO_2\cdots I]^-$ core in $[(CO_2)_2CH_3I]^-$, as discussed later. Figure 6a shows the photoelectron spectrum of $CH_3CO_2^-$ from $[(CO_2)_2CH_3I]^-$ obtained in the photodissociation−photoelectron measurement. The spectrum of acetate, which was formed in the ionized free jet via dissociative electron attachment to acetic anhydride,[16] is also shown for comparison (Figure 6b). The comparison of these two spectra evidently assures the chemical identify of the $CH_3CO_2^-$ photofragment as acetate.

Now the question regarding the electronic structure of $[CH_3CO_2\cdots I]^-$ is how the excess electron is shared between CH_3CO_2 and I. First we consider two extreme cases where the excess electron is localized on one of the constituents, such as $[I^-\cdots CH_3CO_2]$ or $[CH_3CO_2^-\cdots I]$. It seems then worth comparing the photoelectron spectrum of $[CH_3CO_2\cdots I]^-$ with those of I^- and $CH_3CO_2^-$. As seen in the top panel of Figure 5b, the photoelectron spectrum of I^- consists of a pair of sharp "atomic" peaks appearing at 3.06 and 4.00 eV.[28] When I^- forms an ion−neutral complex, these peaks are shifted toward higher electron binding energy but somehow retain their spectral profiles, as in the cases of $I^-(CO_2)$ (see the bottom panel of Figure 5b) and $I^-(N_2O)$.[28] It appears from the results shown in Figure 4 that the $[CH_3CO_2\cdots I]^-$ photoelectron band has broad spectral features. Thus, $[CH_3CO_2\cdots I]^-$ is unlikely to have an electronic structure represented as an ion−neutral complex $[I^-\cdots CH_3CO_2]$. As clearly seen in Figure 6b, the spectral profile of $CH_3CO_2^-$ differs from that of $[CH_3CO_2\cdots I]^-$. Hence, we can rule out the possibility that the excess electron is localized on the acetyloxyl framework as $[CH_3CO_2^-\cdots I]$. These arguments suggest rather the possibility that $[CH_3CO_2\cdots I]^-$ composes a molecular anion and that the excess electron is delocalized to a considerable extent. By considering the fact that the negative charge resides primarily on the O atoms in acetate, we speculate that an O−I bond is formed in $[CH_3CO_2\cdots I]^-$ to share the excess electron.

In order to gain a further insight into the electronic and geometrical structures of $[CH_3CO_2\cdots I]^-$, we have performed *ab initio* calculations. The calculations were carried out at the CCD level with the 6-31+G** basis set for the acetyloxyl group along with the I atom basis set developed by Schwerdtfeger et al.[29] Figure 7 depicts optimized structures for $[CH_3CO_2\cdots I]^-$ and the corresponding neutral CH_3CO_2I. The anion and neutral have an almost identical geometry with the exception of the O−I internuclear distance; $r_{O-I} \approx 2.6$ Å in $[CH_3CO_2\cdots I]^-$ while $r_{O-I} \approx 2.0$ Å in CH_3CO_2I. These results certainly assure that $[CH_3CO_2\cdots I]^-$ is a *molecular anion*. The calculations show the charge delocalization in $[CH_3CO_2\cdots I]^-$, which is consistent with the inference drawn from the experimental data. The singly-occupied molecular orbital (SOMO) accommodating the excess electron arises mainly from the *p* orbitals of I and the adjacent O atom. The elongation of the O−I bond length in $[CH_3CO_2\cdots I]^-$ is ascribed to an antibonding character of the SOMO. The vertical detachment energy of $[CH_3CO_2\cdots I]^-$ is calculated to be 3.56 eV, which is surprisingly in good agreement with the experimental value (3.53 eV).

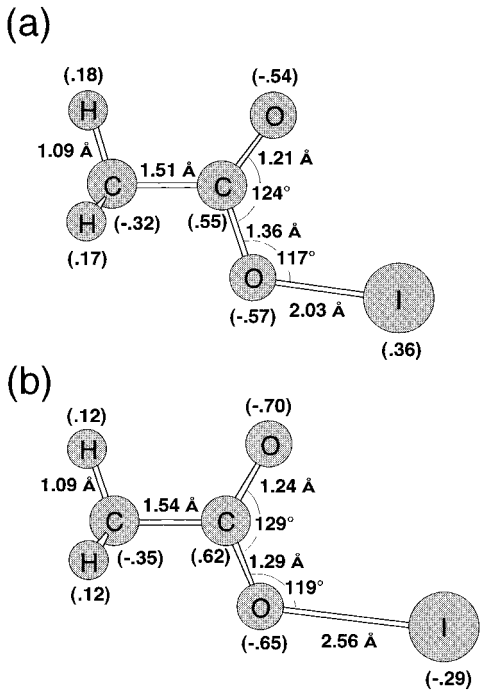

Figure 7. Optimized geometries of (a) acetyloxy iodide and (b) acetyloxy iodide anion obtained with the CCD method. The calculated bond lengths and angles are indicated. Note the significant difference in the O−I bond length between the neutral and anionic species. The number in parentheses represents the charge population at each constituent atom.

It is straightforward to extend the above arguments to $[(CO_2)_nCH_3I]^-$ with $n = 2$ and 3. As shown in Figure 3b,c, $CH_3CO_2^-$, I^-, and $I^-(CO_2)$ are produced in the photodissociation of $[(CO_2)_2CH_3I]^-$ and $[(CO_2)_3CH_3I]^-$ at 532 nm. This shows that $[CH_3CO_2\cdots I]^-$ acts as the chromophoric core in $[(CO_2)_nCH_3I]^-$ with $n = 2$ and 3. It is also interesting to note that additional CO_2 solvent molecules affect the branching ratio between the two photodissociation channels (5a) and (5b) of the $[CH_3CO_2\cdots I]^-$ core. As the I^- and $CH_3CO_2^-$ products must be formed via different potential energy surfaces, this observation is indicative of the solvent-mediated curve crossing operative in the excited states of $[(CO_2)_nCH_3I]^-$. The production of $I^-(CO_2)$ is also suggestive of the CO_2 solvation on the I site of $[CH_3CO_2\cdots I]^-$. The addition of a CO_2 solvent shifts the photoelectron band of $[CH_3CO_2\cdots I]^-$ toward higher binding energy (Table 1). The shift of 0.2−0.3 eV lies in the order of magnitude expected reasonably for an ion−neutral complex $[(CH_3CO_2\cdots I)^-\ (CO_2)_{n-1}]$.

As for the larger $[(CO_2)_nCH_3I]^-$ with $n \geq 7$, the photoelectron spectra can be interpreted by comparing the VDE values of $[(CO_2)_nCH_3I]^-$ with those of $(CO_2)_n^-$. The VDE values of $(CO_2)_n^-$ are reported to be 2.57, 2.73, and 2.80 eV for n = 7−9, respectively.[14] It turns out from the present measurements that an addition of CH_3I to $(CO_2)_n^-$ causes increase in VDE by 0.3−0.45 eV (Table 1) and that the photoelectron band shape of $[(CO_2)_nCH_3I]^-$ is almost identical to that of $(CO_2)_n^-$ with $n \geq 7$, which is well approximated by a Gaussian function having fwhm of 0.7−0.9 eV.[14] From these comparisons, we conclude that $(CO_2)_n^-$ remains intact in $[(CO_2)_nCH_3I]^-$ with $n \geq 7$ as represented by $[(CO_2)_n^-\cdots CH_3I]$. The absence of the photoabsorption band in the larger $[(CO_2)_nCH_3I]^-$ is thus ascribed to the lack of a $[CH_3CO_2\cdots I]^-$ chromophore.

B. Reaction Scheme. The next question to be addressed is how $(CO_2)_N^-$ reacts with CH_3I to form $[CH_3CO_2\cdots I]^-$. The key to this question is the present findings that (1) $[(CO_2)_nCH_3I]^-$ with $n \geq 7$ are *nonreactive* products, which do not contain $[CH_3CO_2\cdots I]^-$, and that (2) the population of $[(CO_2)_nCH_3I]^-$ with n = 4−6 is negligibly small. The formation mechanism of the larger $[(CO_2)_nCH_3I]^-$ with $n \geq 7$ is rather trivial; $(CO_2)_N^-$ picks up one CH_3I, followed by the evaporation of CO_2 solvents:

$$(CO_2)_N^- + CH_3I \rightarrow [(CO_2)_NCH_3I]^{-\dagger} \quad (8)$$

$$[(CO_2)_NCH_3I]^{-\dagger} \rightarrow [(CO_2)_nCH_3I]^- + (N-n)CO_2 \quad (9)$$

The interruption of successive reaction can be explained in terms of the geometrical structures of $(CO_2)_n^-$ with $n \geq 7$. DeLuca et al. have shown by photoelectron spectroscopy that the $(CO_2)_n^-$ clusters in the size range $2 \leq n \leq 5$ have a $C_2O_4^-$ core while a monomer CO_2^- ion forms the core for $n \geq 7$.[14] It should be also noted that the mass spectrum of $(CO_2)_n^-$ displays a magic number at $n = 7$.[3,9,14,15] Therefore it can be inferred that $(CO_2)_n^-$ with $n = 7$ possesses a stable structure where the CO_2^- core is surrounded by a cage of six CO_2 molecules, which forms the first solvent shell.[15] It is likely that this stable shell structure of $(CO_2)_7^-$ prevents CH_3I from approaching the CO_2^- core in $[(CO_2)_nCH_3I]^-$ with $n \geq 7$. We further speculate that CH_3I is adsorbed on the surface of the $(CO_2)_n^-$ clusters. On the other hand, the population of $[(CO_2)_nCH_3I]^-$ in the range $4 \leq n \leq 6$—or rather its absence—suggests that $[(CO_2)_n^-\cdots CH_3I]$ with $n \leq 6$ formed in process 9 is unstable with respect to the successive reaction channels, probably because the solvation shell is unclosed in the smaller cluster size. Then CH_3I easily encounters the $C_2O_4^-$ core, and subsequent reactions occur swiftly:

$$[(CO_2)_n^-\cdots CH_3I] \rightarrow [CH_3CO_2I^-\cdots(CO_2)_{n-1}]^\dagger, \quad n \leq 6 \quad (10)$$

$$[CH_3CO_2I^-\cdots(CO_2)_{n-1}]^\dagger \rightarrow [CH_3CO_2I^-\cdots(CO_2)_{m-1}] + (n-m)CO_2 \quad (11)$$

In process 11 the excess energy of the reaction is consumed by the evaporative loss of CO_2 solvents. We can roughly estimate the number of CO_2 released in process 11 by considering the overall exothermicity for reaction 10, namely

$$\Delta H = D([O_2C{-}CO_2]^-) + \mathrm{EA}(CO_2) + D(H_3C{-}I) - D(H_3C{-}CO_2) - \mathrm{EA}(I) - D([CH_3CO_2{-}I]^-) \quad (12)$$

where EA and D represent electron affinity and bond dissociation energy, respectively. To estimate the value of ΔH, it is assumed, for simplicity, that the solvation energy is same for both reactant and product systems. By using reported values of EA and D ($\mathrm{EA}(CO_2) = -0.60$ eV,[30] $\mathrm{EA}(I) = 3.06$ eV,[23] $D(H_3C{-}I) = 2.47$ eV,[31] and $D(H_3C{-}CO_2) = -0.33$ eV[32]) along with estimated values of $D([O_2C{-}CO_2]^-) = 0.51$ eV[13] and $D([CH_3CO_2{-}I]^-) \approx 0.73$ eV,[33] the heat of reaction is calculated to be $\Delta H \approx -1.08$ eV. As the binding energy of a CO_2 solvent onto the $C_2O_4^-$ core is possibly in the range of 0.22−0.30 eV,[17] a maximum of four or five CO_2 solvents are lost in process 11 due to the exothermicity. The energetics consideration thus explains the absence of $[(CO_2)_nCH_3I]^-$ with $4 \leq n \leq 6$ and the product distribution of $[CH_3CO_2I^-\cdots(CO_2)_{m-1}]$ in the range $1 \leq m \leq 3$.

As only one CO_2 remains in the resulting CH_3CO_2 framework, the cleavage of the C−C bond of the $C_2O_4^-$ core occurs necessarily en route to the final products. Intuitively, the bond breaking of $C_2O_4^-$ is followed by the bond formation of $CH_3CO_2I^-$. This assumption does not certainly exclude the possibility that the reaction proceeds in a concerted manner; the bond breaking and bond formation occur via a $C_2O_4^-\cdot CH_3I$

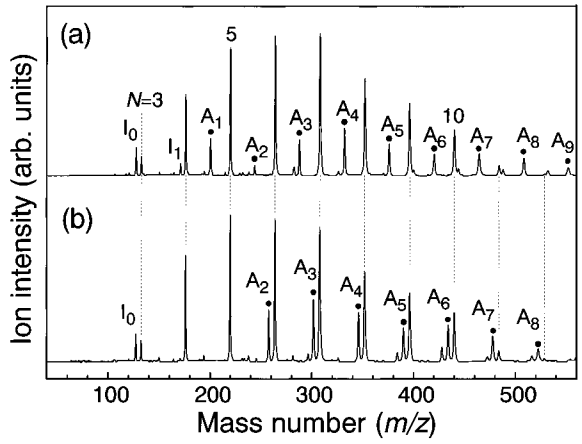

Figure 8. Mass spectra of the product anions in the reaction of $(CO_2)_N^-$ with C_2H_5I (trace a) and with 2-C_3H_7I (trace b). The mass peaks for the product anions are interspersed between the unreacted $(CO_2)_N^-$ peaks. The mass peaks labeled as A_n and I_n correspond to the product anions with the formulae $[(CO_2)_nRI]^-$ (R = C_2H_5, 2-C_3H_7) and $[(CO_2)_nI]^-$, respectively. No product anions having the $[(CO_2)_nR]^-$ formula are observed.

reaction complex prepared in the $[(CO_2)_n^-\cdots CH_3I]$ clusters. Since ≈80% of the excess electron is populated on the carbon atom of CO_2^-,[34] CO_2^- can act as a nucleophilic reagent against CH_3I. In line of this assumption, we have examined steric effects on the reactions, namely, whether or not the reactions are retarded when the reaction site is flanked by methyl groups. Figure 8 shows the mass spectra obtained in the reaction of $(CO_2)_N^-$ with C_2H_5I and with 2-C_3H_7I. In both cases a series of $[(CO_2)_nRI]^-$ (R = C_2H_5, 2-C_3H_7) is observed as the major products:

$$(CO_2)_N^- + C_2H_5I \rightarrow [(CO_2)_nC_2H_5I]^- + (N-n)CO_2 \quad (13)$$

$$(CO_2)_N^- + 2\text{-}C_3H_7I \rightarrow [(CO_2)_n2\text{-}C_3H_7I]^- + (N-n)CO_2 \quad (14)$$

The product distribution of $[(CO_2)_nC_2H_5I]^-$ is prominent at $n = 1$ but otherwise shows a smooth distribution. The $[(CO_2)_n2\text{-}C_3H_7I]^-$ products are populated without any intensity anomalies, starting at $n = 2$. The photodissociation measurements show that $[(CO_2)C_2H_5I]^-$ has a form of $[C_2H_5CO_2\cdots I]^-$, because it dissociates into $C_2H_5CO_2^-$ or I^- at 532 nm photoexcitation (Figure 9a). The small intensities of the photofragments from $[(CO_2)_2C_2H_5I]^-$ (Figure 9b) indicate that a tiny portion of $[(CO_2)_2C_2H_5I]^-$ has the $[C_2H_5CO_2\cdots I]^-$ core, while most of $[(CO_2)_2C_2H_5I]^-$ are nonreactive products having a form of $[(CO_2)_2^-\cdots C_2H_5I]$. The larger $[(CO_2)_nC_2H_5I]^-$ with $n \geq 3$ do not photodissociate at 532 nm (Figure 9c); $[C_2H_5CO_2\cdots I]^-$ is no longer a core of $[(CO_2)_3C_2H_5I]^-$. The measurements also reveal that almost none of $[(CO_2)_n2\text{-}C_3H_7I]^-$ contains a $[2\text{-}C_3H_7\text{-}CO_2\cdots I]^-$ chromophore (Figure 9d,e). These inferences deduced from the results shown in Figure 9 are further confirmed by the measurements of photoelectron spectra of $[(CO_2)_nC_2H_5I]^-$ and $[(CO_2)_n2\text{-}C_3H_7I]^-$. All the photoelectron spectra of $[(CO_2)_nC_2H_5I]^-$ and $[(CO_2)_n2\text{-}C_3H_7I]^-$, except for $[(CO_2)C_2H_5I]^-$, display photoelectron bands assignable to $[(CO_2)_n^-\cdots RI]$. As a measure of reactivity, the percentage populations of the reactive products are estimated as $\sum_n I\{[RCO_2I^-\cdots(CO_2)_{n-1}]\}/\sum_n I\{[(CO_2)_nRI]^-\}$, where $I\{...\}$ represents the intensity of each mass peak. The percentage populations are calculated to be 70% for CH_3I, 12% for C_2H_5I, and ≈0% for 2-C_3H_7I. These values clearly exhibit the effects of steric hindrance; the reactivity is retarded when the number of methyl groups

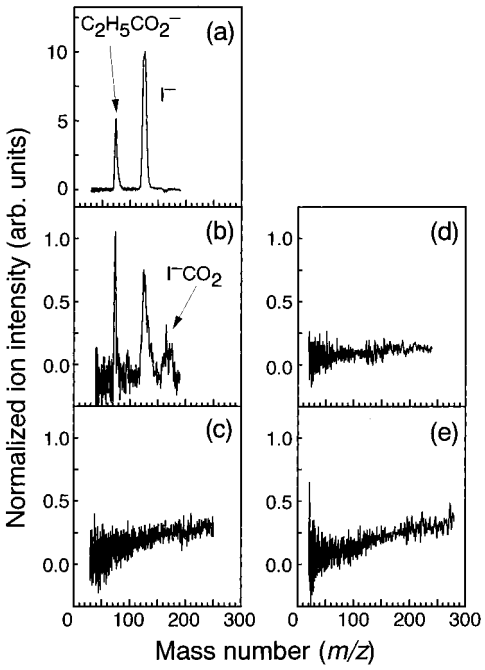

Figure 9. Photofragment mass spectra resulting from the 532-nm photodissociation of $[(CO_2)_nC_2H_5I]^-$ (a) $n = 1$; (b) $n = 2$; (c) $n = 3$ and $[(CO_2)_n2\text{-}C_3H_7I]^-$ (d) $n = 2$; (e) $n = 3$. Each peak intensity is normalized with the laser power and the parent ion intensity. The ordinate scale is given such as to assign 10 units to the largest experimental peak.

SCHEME 1

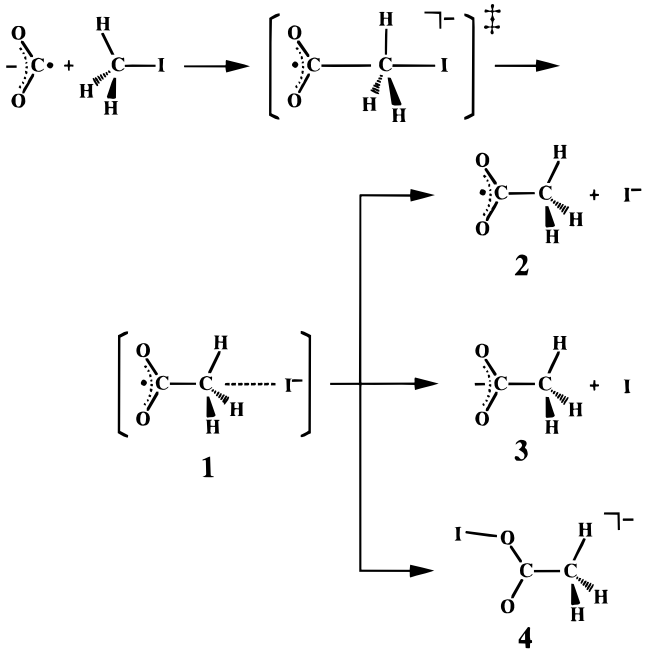

surrounding the reaction center increases. Hence, we conclude that the attack of $^\bullet CO_2^-$ occurs on the C atom from the hindered side of alkyl iodide and that the reaction proceeds as a bimolecular nucleophilic substitution (S_N2). Within the framework of the S_N2 scheme, $CH_3CO_2I^-$ is formed via Scheme 1. Here the essence of the reaction within the clusters is described. When the reaction proceeds along the S_N2 pathway via the radical−ion complex (species **1**) to product **2**, I^- acts as a leaving group, and as a result, $I^-(CO_2)_n$ is formed. In fact, $I^-(CO_2)_n$ ($0 \leq n \leq 4$) is observed in the product mass spectra, although $I^-(CO_2)_n$ might be produced also through the side processes (process 2). As the electron affinity of acetyloxyl

radical is accidentally quite close to that of iodine atom, electron transfer might happen between CH_3CO_2 and the leaving I^- atom. This leads to the production of $[CH_3CO_2^-(CO_2)_{n-1}]$ (species **3**), which is also detected in the mass spectrum as $[(CO_2)_nCH_3]^-$. By comparing the photoelectron spectrum of $[(CO_2)_2CH_3]^-$ (the top panel of Figure 5a) with that of acetate (Figure 6b), it can be inferred that acetate forms the anionic core of $[(CO_2)_nCH_3]^-$. From species **1** to the main product (species **4**), the iodine atomic anion, which is the leaving group of S_N2, possibly migrates within the clusters to form the most stable molecular anion $CH_3CO_2I^-$.

Conclusion

In summary, we report on the reactions of $(CO_2)_N^-$ with CH_3I. Not only mass spectrometry but photoelectron spectroscopy, photodissociation measurement, and their combination are used to probe the product anions. The main conclusions drawn from the present study are summarized as follows:

(1) Negatively-charged clusters of carbon dioxide $(CO_2)_N^-$ react with CH_3I leading to the formation of anions with the formulae $[(CO_2)_nCH_3I]^-$, $[(CO_2)_nCH_3]^-$, and $[(CO_2)_nI]^-$. At first glance the product anions $[(CO_2)_nCH_3I]^-$ appear to arise from the adsorption of CH_3I onto $(CO_2)_N^-$. However, close examination has revealed that an acetyloxy iodide anion, $CH_3CO_2I^-$, is formed in $[(CO_2)_nCH_3I]^-$ with $1 \leq n \leq 3$. The bimodal behavior of the product distribution indicates that the reaction is inherent in the smaller $(CO_2)_N^-$ clusters with size $N \leq 6$.

(2) The $CH_3CO_2I^-$ anion exhibits a large VDE value of 3.53 eV, due probably to the delocalization of the excess electron. *Ab initio* calculations show that the excess electron resides in the O−I antibonding orbital of $CH_3CO_2I^-$.

(3) The reaction is strongly subject to steric hindrance around the carbon site of alkyl iodide. In fact, the reaction of $(CO_2)_N^-$ with 2-C_3H_7I yields no product cluster anions containing a 2-$C_3H_7CO_2I^-$ core. We infer from this finding that $CH_3CO_2I^-$ is formed via an S_N2 transition state, which is prepared by a nucleophilic attack of CO_2^- on the carbon site of alkyl iodide.

Thus, we have demonstrated for the first time the chemical reactivity of $(CO_2)_N^-$ as a nucleophile in the gas-phase reaction. The overall reaction process can be regarded as carboxylation by the reductive activation of CO_2, which opens up a possibility of studying elementary processes of electrochemical reactions, not in the condensed phase but in the gas phase with a restricted number of solvent molecules.

Acknowledgment. The authors are grateful to Professor A. Nakajima for his helpful advice on the design of the photoelectron spectrometer. They are also indebted to Dr. Jan Hrušák for his helpful comments on the *ab initio* calculations. Professor A. Onaka is also acknowledged for valuable discussions regarding the reaction scheme. This work was supported partly by a Grant-in-Aid for Scientific Research from the Ministry of Education, Science and Culture. The financial support of the Multi-disciplinary Science Foundation, the Sumitomo Foundation, and the Matsuo Foundation is also gratefully acknowledged.

References and Notes

(1) Klots, C. E.; Compton, R. N. *J. Chem. Phys.* **1977**, *67*, 1779; **1978**, *69*, 1636.

(2) Stamatovic, A.; Leiter, K.; Ritter, W.; Stephan, K.; Märk, T. D. *J. Chem. Phys.* **1985**, *83*, 2942.

(3) Knapp, M.; Kreisle, D.; Echt, O.; Sattler, K.; Recknagel, E. *Surf. Sci.* **1985**, *156*, 313.

(4) Kondow, T.; Mitsuke, K. *J. Chem. Phys.* **1985**, *83*, 2612.

(5) Knapp, M.; Echt, O.; Kreisle, D.; Märk, T. D.; Recknagel, E. *Chem. Phys. Lett.* **1986**, *126*, 225.

(6) Tsukada, M.; Shima, N.; Tsuneyuki, S.; Kageshima, H.; Kondow, T. *J. Chem. Phys.* **1987**, *87*, 3927.

(7) Kondow, T. *J. Phys. Chem.* **1987**, *91*, 1307.

(8) Haberland, H.; Ludewigt, C.; Schindler, H.-G.; Worsnop, D. R. In *Large Finite Systems*; Jortner, J., Pullman, A., Pullman, B., Eds.; Dordrecht: Reidel, 1987; p 195.

(9) Quitevis, E. L.; Herschbach, D. R. *J. Phys. Chem.* **1989**, *93*, 1136.

(10) Kraft, T.; Ruf, M.-W.; Hotop, H. *Z. Phys.* **1989**, *D14*, 179.

(11) Misaizu, F.; Mitsuke, K.; Kondow, T.; Kuchitsu, K. *J. Chem. Phys.* **1991**, *94*, 243.

(12) Fleischman, S. H.; Jordon, K. D. *J. Phys. Chem.* **1987**, *91*, 1300.

(13) Bowen, K. H.; Eaton, J. G. In *The Structure of Small Molecules and Ions*; Naaman, R., Vagar, Z., Eds.; Plenum Press: New York, 1987; p 147.

(14) DeLuca, M. J.; Niu, B.; Johnson, M. A. *J. Chem. Phys.* **1988**, *88*, 5857.

(15) Tsukuda, T.; Johnson, M. A.; Nagata, T. *Chem. Phys. Lett.* **1997**, *268*, 429.

(16) Cooper, C. D.; Compton, R. N. *Chem. Phys. Lett.* **1972**, *14*, 29; *J. Chem. Phys.* **1973**, *59*, 3550.

(17) Alexander, M. L.; Johnson, M. A.; Levinger, N. E.; Lineberger, W. C. *Phys. Rev. Lett.* **1986**, *57*, 976.

(18) Hirokawa, J. Ph.D. Dissertation, The University of Tokyo, 1993.

(19) Neta, P.; Huie, R. E.; Ross, A. B. *J. Phys. Chem. Ref. Data* **1987**, *17*, 1027.

(20) Tyssee, D. A.; Wagenknecht, J. H.; Baizer, M. M.; Chruma, J. L. *Tetrahedron Lett.* **1972**, *47*, 4809.

(21) Tsukuda, T.; Saeki, M.; Nagata, T. *Chem. Phys. Lett.* **1996**, *251*, 309.

(22) Caldwell, G.; Rennenboog, R.; Kebarle, P. *Can. J. Chem.* **1989**, *67*, 611.

(23) Hotop, H.; Lineberger, W. C. *J. Phys. Chem. Ref. Data* **1985**, *14*, 731.

(24) Johnson, M. A.; Lineberger, W. C. In *Techniques in Chemistry*, Farrar, J. M., Saunders, W. H., Eds.; Wiley: New York, 1988; Vol. 20, p 591.

(25) Kruit, P.; Read, F. H. *J. Phys.* **1983**, *E16*, 313.

(26) Cha, C.-Y.; Gantefor, G.; Eberhardt, W. *Rev. Sci. Instrum.* **1992**, *63*, 5661.

(27) Nakajima, A.; Taguwa, T.; Hoshino, K.; Sugioka, T.; Naganuma, T.; Ono, F.; Watanabe, K.; Nakao, K.; Konishi, Y.; Kishi, R.; Kaya, K. *Chem. Phys. Lett.* **1993**, *214*, 22.

(28) Arnold, D. W.; Bradforth, S. E.; Kim, E. H.; Neumark, D. M. *J. Chem. Phys.* **1995**, *102*, 3493, 3510.

(29) Schwerdtfeger, P.; Dolg, M.; Schwarz, W. H. E.; Bowmaker, G. A.; Boyd, P. D. W. *J. Chem. Phys.* **1989**, *91*, 1762.

(30) Compton, R. N.; Reinhardt, P. W.; Cooper, C. D. *J. Chem. Phys.* **1975**, *63*, 3821.

(31) *CRC Handbook of Chemistry and Physics*; Weast, R. C., Astle, M. J., Eds.; CRC Press: Boca Raton, FL, 1988−89.

(32) The bond dissociation energy $D(CH_3-CO_2)$ is estimated from the reported values of the heat of formation of CH_3, CO_2, and CH_3CO_2; $\Delta H(CH_3) = 1.508$ eV, $\Delta H(CO_2) = -4.078$ eV, $\Delta H(CH_3CO_2) = -2.24$ eV.

(33) Saeki, M.; Nagata, T. Unpublished data.

(34) Pacansky, J.; Wahlgren, U.; Bagus, P. S. *J. Chem. Phys.* **1975**, *62*, 2740.